JOURNAL OF PLANKTON RESEARCH | VOLUME 26 | NUMBER 8 | PAGES 885–900 | 2004

Light rather than iron controls photosynthate production and allocation in Southern Ocean phytoplankton populations during austral autumn

T. VAN OIJEN[1,*], M. A. VAN LEEUWE[1], E. GRANUM[2], F. J. WEISSING[3], R. G. J. BELLERBY[4], W. W. C. GIESKES[1] AND H. J. W. DE BAAR[1,5]

[1]DEPARTMENT OF MARINE BIOLOGY, CEES, UNIVERSITY OF GRONINGEN, PO BOX 14, 9750 AA HAREN, THE NETHERLANDS, [2]DEPARTMENT OF ANIMAL AND PLANT SCIENCES, UNIVERSITY OF SHEFFIELD, SHEFFIELD S10 2TN, UK, [3]THEORETICAL BIOLOGY, UNIVERSITY OF GRONINGEN, PO BOX 14, 9750 AA HAREN, THE NETHERLANDS, [4]BJERKNES CENTRE FOR CLIMATE RESEARCH, UNIVERSITY OF BERGEN, ALLÉGATEN 55, 5007 BERGEN, NORWAY AND [5]THE ROYAL NETHERLANDS INSTITUTE FOR SEA RESEARCH, PO BOX 59, 1790 AB DEN BURG, THE NETHERLANDS

*CORRESPONDING AUTHOR: t.van.oijen@biol.rug.nl

Received November 17, 2003; accepted in principle March 3, 2004; accepted for publication April 15, 2004; published online April 30, 2004

The role of iron and light in controlling photosynthate production and allocation in phytoplankton populations of the Atlantic sector of the Southern Ocean was investigated in April–May 1999. The ^{14}C incorporation into five biochemical pools (glucan, amino acids, proteins, lipids and polysaccharides) was measured during iron/light perturbation experiments. The diurnal Chl a-specific rates of carbon incorporation into these pools did not change in response to iron addition, yet were decreased at 20 μmol photons m^{-2} s^{-1}, an irradiance comparable with the one at 20–45 m in situ depth. This suggests that the low phytoplankton biomass encountered (0.1–0.6 μg Chl a L^{-1}) was mainly caused by light limitation in the deep wind mixed layer (>40 m). Regional differences in Chl a-specific carbon incorporation rates were not found in spite of differences in phytoplankton species composition: at the Antarctic Polar Front, biomass was dominated by a diatom population of Fragilariopsis kerguelensis, whereas smaller cells, including chrysophytes, were relatively more abundant in the Antarctic Circumpolar Current beyond the influence of frontal systems. Because mixing was often in excess of 100 m in the latter region, diatom cells may have been unable to fulfil their characteristically high Fe demand at low average light conditions, and thus became co-limited by both resources. Using a model that describes the ^{14}C incorporation, the consistency was shown between the dynamics in the glucan pool in the field experiments and in laboratory experiments with an Antarctic diatom, Chaetoceros brevis. The glucan respiration rate was almost twice as high during the dark phase as during the light phase, which is consistent with the role of glucan as a reserve supplying energy and carbon skeletons for continued protein synthesis during the night.

INTRODUCTION

The Southern Ocean consists of several distinct provinces that differ in many physical and chemical parameters including temperature, minor and major nutrient concentrations, light availability, sea ice formation, currents and vertical mixing (Jacques, 1989; Boyd, 2002). Frontal systems, such as the Antarctic Polar Front, are generally characterized by high phytoplankton biomass whereas in other regions, like the Antarctic Circumpolar Current beyond the influence of frontal systems, biomass is low (Lutjeharms *et al.*, 1985; Laubscher *et al.*, 1993; Bracher *et al.*, 1999). Understanding how marine phytoplankton productivity is controlled is important because algal carbon fixation in the ocean is a link between the atmospheric and

doi: 10.1093/plankt/fbh088, available online at www.plankt.oupjournals.org

oceanic compartment of the global carbon cycle (Falkowski *et al.*, 1998). Specifically, diatom blooms in the Southern Ocean are assumed to be followed by a significant export flux of carbon out of the euphotic zone and carbon dioxide (CO_2) drawdown (De Baar and Boyd, 2000).

Over the past two decades, iron availability has been identified as a major factor controlling phytoplankton growth in the Southern Ocean. At limiting iron concentrations the functioning of the photosynthetic apparatus and several metabolic processes are affected (Geider and La Roche, 1994). Differences in iron availability may explain the difference in productivity between frontal systems and other regions of the Antarctic Circumpolar Current during austral spring (De Baar *et al.*, 1995). Moreover, there are indications of further seasonal progression in the environmental control of phytoplankton (Boyd, 2002). This commences with irradiance as the sole controlling factor in early spring (Tilzer *et al.*, 1985). During early summer, *in situ* measurements combined with modelling suggest that phytoplankton productivity is co-limited by iron and light (Lancelot *et al.*, 2000). During mid-summer, results of field surveys, mesocosm experiments and an *in situ* iron fertilization experiment point to iron availability as the crucial factor controlling diatom bloom formation (De Baar *et al.*, 1995; Boyd *et al.*, 2000). For some regions a simultaneous limitation of iron and silicic acid has been proposed (Franck *et al.*, 2000; Hutchins *et al.*, 2001; Nelson *et al.*, 2001).

The aim of this study was to investigate the role of iron and light availability for carbon fixation by phytoplankton in the Atlantic sector of the Southern Ocean during austral autumn. Little is known about the environmental controls in this season, yet especially at this time of year blooms may end in mass sedimentation of phytoplankton cells and carbon export (Smetacek, 2000). We focussed our research on the patterns of photosynthate allocation into five different biochemical pools, including a pool of storage carbohydrates. These carbohydrates play a key role in cell growth in a variable light climate by the provision of energy and carbon skeletons for continued protein synthesis in darkness (Cuhel *et al.*, 1984; Granum and Myklestad, 2001). The production of storage carbohydrates is strongly light-dependent and exhibits diel dynamics in healthy growing phytoplankton exposed to a day–night cycle (Hitchcock, 1980; Vårum *et al.*, 1986). We hypothesize that if cells are iron-limited in the field, addition of iron will lead to an increase in the diurnal carbon incorporation into the pool of storage carbohydrates.

We tested this hypothesis using 24 h mesocosm experiments at two relevant photon flux densities. The experiments were preceded by a one-day adaptation period to added Fe which should be sufficiently long to see a response in phytoplankton photosynthesis rates. Indeed, an increase in the quantum yield of photosynthesis (F_v/F_m) has always been observed within a day after Fe addition during *in situ* fertilization experiments in the Antarctic Ocean (Boyd and Abraham, 2001; Barber, 2002; Gervais *et al.*, 2002) and elsewhere (Behrenfeld *et al.*, 1996). This increase is directly reflected in the rate of carbon fixation measured by ^{14}C incubations (Kolber *et al.*, 1994; Maldonado *et al.*, 1999; Davey and Geider, 2001). The advantage of short incubations over longer ones (days to weeks) is that a potential shift in the phytoplankton community composition is avoided. Therefore, results are indicative of the performance of the resident community.

Photosynthate allocation was determined by biochemical fractionation of incorporated ^{14}C into different carbon pools. This approach has been introduced in phytoplankton research by Morris *et al.* (Morris *et al.*, 1974). For a better isolation of water-extractable storage carbohydrates (glucan), we adapted the method described by Granum and Myklestad (Granum and Myklestad, 2001). Because this fractionation method had never before been used in the field, we performed additional laboratory experiments with single-species cultures of an Antarctic diatom to study the dynamics in the different fractions and compare ^{14}C incorporation into glucan with results of chemical analysis (no Fe limitation).

METHOD

Experimental set-up

Field experiments

Research was conducted during the R.V. 'Polarstern' ANT 16/3 expedition in the Atlantic sector of the Southern Ocean, during April–May 1999. The study area comprised three different provinces: the Antarctic Polar Front, the Antarctic Circumpolar Current beyond the influence of frontal systems, and the marginal ice zone (Figure 1, Table I). Seawater was sampled from 60 m depth with a rosette sampler with Kevlar wire at eight stations using trace metal clean techniques; subsamples were taken for cell counts, chlorophyll (Chl) *a* concentration and total dissolved iron concentration. The seawater samples were incubated under ultra-clean conditions in 20 L bottles in a container at ambient temperature (4 ± 2°C) and light regime (12:12 h light:dark) and a photon irradiance of 90 μmol photons m^{-2} s^{-1}, with and without addition of 2 nM iron. After an acclimation period of at least a full light–dark period, the response of the phytoplankton over one light–dark

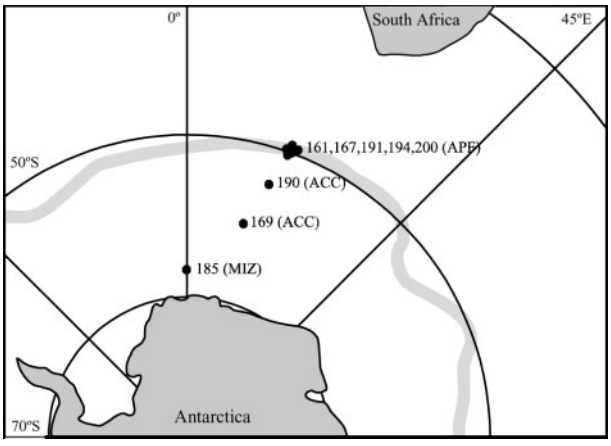

Fig. 1. Sampling locations (filled circles) during ANT 16/3 of RV Polarstern in the Atlantic sector of the Southern Ocean. Numbers refer to station numbers. APF, Antarctic Polar Front; ACC, Antarctic Circumpolar Current outside of frontal systems; MIZ, Marginal Ice Zone. The grey band indicates the approximate location of the Antarctic Polar Front.

period was examined. Control and iron-enriched subsamples were spiked at dawn with ^{14}C carbonate (2.0–8.9 MBq L^{-1}) and incubated in 250 mL polycarbonate bottles at low light (LL, 20 μmol photons m^{-2} s^{-1}) and at high light conditions (HL, 90 μmol photons m^{-2} s^{-1}). For each treatment, five times an entire bottle was sampled at 4–6 h intervals. The total dissolved inorganic carbon (TCO_2) concentration was measured in samples taken near the surface or in the upper water column at the same stations.

For the high irradiance, part of the sample was also incubated without the addition of ^{14}C carbonate for further chemical analysis. At the beginning and the end of the light period, samples were taken for Chl *a* concentration, the concentration of water-extractable carbohydrates in the particulate fraction, and the monosaccharide composition of these carbohydrates.

Laboratory experiment

Two cultures of the Antarctic diatom *Chaetoceros brevis* (CCMP 163) were grown separately for several months in filtered (0.2 μm) natural seawater, enriched with major nutrients, trace elements and vitamins in concentrations of Guillard's f/2 medium (Guillard, 1975), within a controlled 6 ± 2°C cabinet at a 12:12 h light:dark regime. Illumination was provided by a rack of alternating Philips TLD 18W/33 and TLD 18W/96 tubes with an irradiance of 100 μmol photons m^{-2} s^{-1}, measured by a Biospherical Instruments (San Diego, CA, USA) QSL-100 light meter. One week before the experiment each culture was used to inoculate 1 L of seawater medium and cultured at the same conditions. These cultures were growing exponentially at a rate (μ) of 0.54 ± 0.03 day^{-1} and at the start of the experiment they reached a density of 768 000 ± 57 000 cells mL^{-1}. At t = 0, each of the cultures was distributed over six 200 mL glass Erlenmeyer flasks: one for a 'long-term' ^{14}C incubation, four for 'cumulative short-term' ^{14}C incubations, and one for a long-term incubation without ^{14}C addition. The long-term ^{14}C incubations were performed over a full light–dark period (24 h). The ^{14}C carbonate was added at the start of the light period at 0.4 MBq L^{-1}. At 3 h intervals, 5 mL samples were taken for total and biochemically fractionated ^{14}C incorporation. During the light period only, cumulative short-term ^{14}C incubations were performed in order to estimate the gross rates of carbon incorporation into the different pools and compare it with the rates estimated from the long-term incubations. At t = 0, 3, 6 and 9 h, a culture

Table I: Overview of initial parameters of the incubation experiments for the sample locations: the Antarctic Polar Front (APF), the Antarctic Circumpolar Current (ACC) beyond the influence of frontal systems, and the marginal ice zone (MIZ)

Exp.	Date	Station	Location	Region	Chl *a* (μg L^{-1})	POC (μg L^{-1})	Cells (mL^{-1})	[Si] (μM)	[NO_3] (μM)	[PO_4] (μM)	[Fe] (nM)
1	3 April 1999	161	50°00′S 19°04′E	APF	0.60	103	542	16.1	24.0	1.52	n.d.[a]
2	6 April 1999	167	49°50′S 20°00′E	APF	0.28	55	326	5.4	23.7	1.34	0.68
6	27 April 1999	191	49°22′S 20°34′E	APF	0.30	67	287	10.4	23.9	1.42	0.22
7	29 April 1999	194	49°22′S 20°02′E	APF	0.30	66	275	9.0	23.3	1.45	0.56
8	4 May 1999	200	50°00′S 20°01′E	APF	0.44	68	425	15.8	22.6	1.45	0.15
3	9 April 1999	169	60°00′S 18°32′E	ACC	0.15	53	239	44.5	23.2	1.62	0.37
5	25 April 1999	190	54°02′S 20°00′E	ACC	0.27	67	150	57.6	26.2	1.71	0.47
4	21 April 1999	185	66°59′S 00°03′E	MIZ	0.07	42	103	64.6	27.1	1.75	0.21

[a]Not determined.

was spiked with ^{14}C carbonate at 0.4 MBq L^{-1} and after 3 h, 5 mL samples were taken for total and fractionated ^{14}C incorporation. Finally, from the culture that was not spiked with ^{14}C, samples were taken for water-extractable carbohydrates in the particulate fraction at 3 h intervals. Samples for the TCO_2 concentration were taken at the beginning and the end of the experiment.

Analyses

Major nutrient analyses

The concentrations of nitrate, phosphate and silicate were determined on board using a Technicon II Autoanalyser following standard methods (Hartmann *et al.*, 2000).

Iron analyses

Samples were acidified to pH <2 with ultraclean quartz distilled concentrated nitric acid. Total dissolvable iron (unfiltered) was measured onboard using a flow injection technique with inline pre-concentration on a chelating resin followed by chemiluminescence detection (FIA-CL) (De Jong *et al.*, 1998).

Chl a analyses

Immediately after sampling, 1000 mL samples were filtered on a Whatman GF/F filter. The filters were ground in 10 ml 90% acetone, extracted at 4°C for 2 h, and centrifuged. The extract fluorescence was measured before and after acidification with 1 N HCl using a Turner Design Model 10-AU digital fluorometer. The Chl *a* concentration was calculated according to Arar and Collins (Arar and Collins, 1992).

Cell numbers and species composition

Cell numbers in the laboratory cultures were determined with a Bürker hemocytometer as the mean of four counts with a coefficient of variation of 5–10%. For cell numbers and species composition in field samples, 250 mL samples were preserved in lugol of 0.5% final concentration. Cell counts and biovolumetric estimates were done on an inverted microscope (Olympus IMT-2), with at least 200 observations per sample. The biovolume was calculated by means of a species-specific function for the relationship between the cell volume and the length or diameter of the cell, which were measured with an ocular micrometer (Koeman, 1999).

Carbohydrate analyses

Samples of 10 mL (laboratory cultures) to 4000 mL (field samples) were filtered through pre-combusted (350°C) 25 mm GF/F Whatman filters under gentle vacuum pressure (<200 mm Hg). The filters were stored at −20°C until analysis. They were extracted in water (Milli-Q) in sealed glass test tubes placed in a water bath for 1 h at 80°C. Afterwards, the tubes were cooled and centrifuged for 5 min at 715 *g*. The total carbohydrate concentration and the mono- and polysaccharide concentration in the extracts were determined with the colorimetric TPTZ-method described by Myklestad *et al.* (Myklestad *et al.*, 1997), with minor modifications. D(+)-glucose was used as the standard.

Neutral aldose composition analysis

Part of the hot water extracts was freeze-dried (Labconco Freezone 4.5). Subsequently, the aldose composition was determined according to Kamerling and Vliegenthart (Kamerling and Vliegenthart, 1989). Briefly, the samples were subjected to methanolysis (1.0 M methanolic HCl, 24 h, 85°C) prior to the analysis of the trimethylsilylated (N-reacetylated) methyl glycosides on a gas chromatograph (Varian 3600) equipped with a 0.32 mm diameter, 30 m length capillary column (DB-1, J & W Scientific) and a flame ionization detector (FID). Identification and calculation of relative composition of sugar derivatives were performed by comparison with standards (Sigma). Arabinose could not be analysed due to peak interference.

TCO_2 analysis

For the culture experiment, samples were filtered over a Whatman GF/F filter. The filtrate was analysed on a Tekmar-Dohrmann Apollo 9000 carbon analyser with Na_2CO_3 as an internal standard. After acidification to pH 2, samples were sparged with inert gas (high quality CO_2-free synthetic air), and produced CO_2 was swept through a moisture control system and a halogen scrubber. The CO_2 concentration was measured using an infrared detector.

For field samples the TCO_2, i.e. the sum of all carbonate species, was determined with the coulometric method after Johnson *et al.* (Johnson *et al.*, 1987) as slightly modified by Robinson and Williams (Robinson and Williams, 1992) and Stoll (Stoll, 1994). Standards [certified reference material (DOE, 1994) made available by Prof. A. Dickson of the Scripps Institution of Oceanography] were measured for each cell prepared for the coulometer and the cells were changed about once a day.

Biochemical fractionation of incorporated ^{14}C

The samples (field: 225 mL, lab: 5 mL) were filtered on pre-combusted (350°C) 25 mm GF/F filters under gentle vacuum (50 mm Hg) and purged of inorganic ^{14}C by acidification (exposing the filters to concentrated HCl vapour in a vacuum exsiccator for 30 min) and stored at −20°C. Biochemical fractionation was performed by a modification of the method of Li *et al.* (Li *et al.*, 1980) with additional separation of the 'low-molecular-weight'

(low-MW) fraction into a basic fraction (including amino acids, purines, pyrimidines) denoted 'amino acids' and an acid/neutral fraction (including β-1,3-glucan, monosaccharides, organic acids) denoted 'glucan' (Granum and Myklestad, 1999, 2001). The sum of the calculated amounts of ^{14}C in all biochemical fractions was on average 98% of the measured total amount of ^{14}C fixed. The inorganic carbon assimilation rate (dC/dt) was calculated according to Geider and Osborne (Geider and Osborne, 1992):

$$\frac{dC}{dt} = f\frac{d^{14}C}{dt}\frac{C_{med}}{^{14}C_{med}} \quad (1)$$

where $d^{14}C/dt$ is the rate of ^{14}C fixation, $^{14}C_{med}$ is the total amount of ^{14}C added to the culture (the total activity of $NaH^{14}CO_3$ divided by the specific activity), C_{med} is the TCO_2 concentration and f is the carbon isotope discrimination factor (1.06).

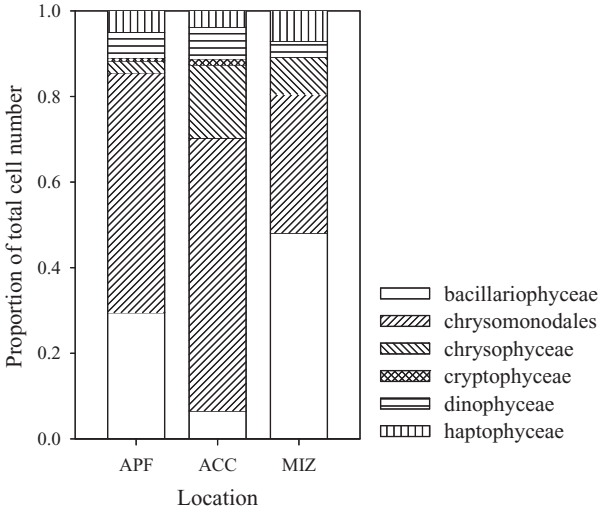

Fig. 2. Species composition at the APF, the ACC outside fronts and the MIZ. Chrysomonadales is a semi-taxonomic group of small phytoplankton cells that could not be assigned to a class.

RESULTS

Field experiments

General

The different regions studied were distinct in the concentrations of major nutrients, especially of silicic acid which was up to 70 μM at the marginal ice zone (MIZ) and as low as 5 μM at the Antarctic Polar Front (APF) (Hartmann *et al.*, 2000). In correspondence, in experiments performed at the APF the initial silicic acid concentrations were lowest, 5.4–16.1 μM, compared with 44.5–57.6 and 65 μM in experiments performed in the Antarctic Circumpolar Current beyond the influence of frontal systems (hereafter simply ACC) and at the MIZ, respectively (Table I). Nitrate concentrations were high in all regions and varied between 24–28 μM in the experiments; phosphate concentrations were 1.4–1.8 μM. Dissolved iron concentrations in the research area varied between 0.05–0.80 nM, being slightly higher at the APF (De Baar and De Jong, 2001). For the experiments, initial concentrations were 0.15–0.68 nM without a clear difference between the experiments of the different regions.

The Chl *a* concentration varied between 0.3–0.6 μg L^{-1} in APF experiments, between 0.15–0.27 in ACC experiments and was 0.07 for the experiment performed with MIZ water (Table I). Total phytoplankton cell counts varied from 100 000 to 500 000 cells L^{-1} (Table I). There were distinct differences in species composition between the different geographic regions (Figure 2). At the APF the phytoplankton community was dominated by diatoms (bacillariophyceae), at an abundance up to 190 000 cells L^{-1}, thereby contributing 30% to the total cell number and 90% to the total biovolume. The most abundant diatom species was *Fragilariopsis kerguelensis*, followed by *Pseudo-nitzschia* sp. and *Chaetoceros* sp. A more detailed overview of the species composition at the APF during the same cruise has been presented by Van Oijen *et al.* (Van Oijen *et al.*, 2003). Diatom abundance was much lower in ACC waters (<15 000 cells L^{-1}) where they contributed <10% to the total cell number but nevertheless 70% of the total biovolume. Here, small chrysophytes, chrysomonadales and Dinophyceae were numerically dominant. At the MIZ, the low phytoplankton abundance was dominated by diatoms which contributed 50% to the total cell number and >95% to the total biovolume. Haptophyceae, mostly *Phaeocystis* sp., were proportionally more abundant at the APF and the MIZ than in the ACC (Figure 2). The difference in species composition between regions was reflected in the average cell volume: 1800 μm^3 and 2500 μm^3 for APF and MIZ where large diatoms were dominant and only 500 μm^3 for the ACC.

Patterns of carbon incorporation showed only minor differences between regions. Below we provide a detailed description of these patterns for one region, the APF, and subsequently make a brief comparison with the other regions.

Carbon incorporation at the APF

The diurnal carbon incorporation rate in incubations performed with phytoplankton sampled at the APF was strongly dependent on irradiance but did not change in response to Fe addition for any of the pools (Figure 3A–E). The net diurnal production rate of

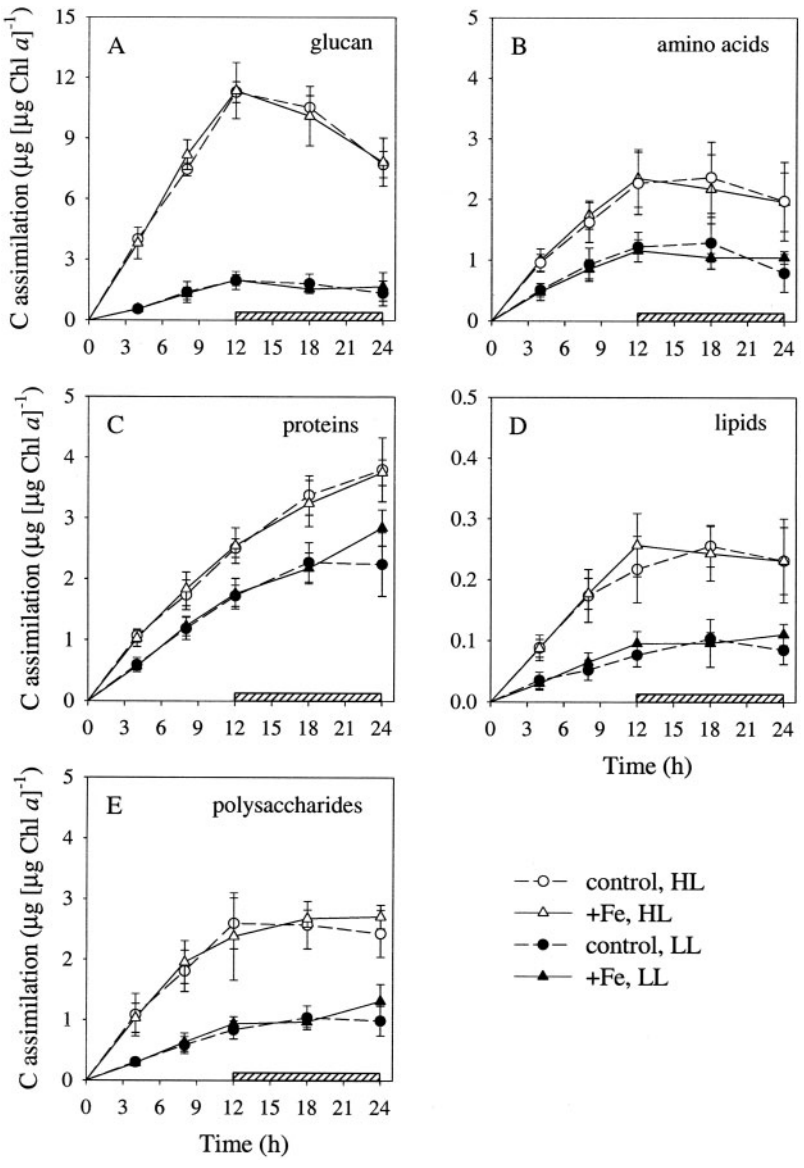

Fig. 3. The ^{14}C incorporation into the biochemical pools (**A**) glucan, (**B**) amino acids, (**C**) proteins, (**D**) lipids and (**E**) polysaccharides during long-term (24 h) incubations with natural phytoplankton populations of the APF at low and high photon irradiance, with and without the addition of iron. Error bars indicate standard deviations (n = 5). HL, high light; LL, low light. Dashed bars indicate the dark period.

glucan was almost 6 times higher at high compared with low irradiance (Table II). In contrast, the diurnal carbon incorporation rates into proteins and amino acids were less than two times higher. Thus, the relative incorporation into the different fractions was strongly dependent on the irradiance. At high irradiance 60% of the total carbon fixed was incorporated into glucan during the light period, whereas at low irradiance it was only 33%. The glucan fraction showed strongest diel dynamics and decreased at night, whereas protein synthesis continued during the dark period at both high and low photon irradiance. Consequently, the relative contribution of glucan decreased to 48 and 24% at high and low irradiance, respectively. The levels of carbon incorporated into amino acids, lipids and polysaccharides remained relatively constant over the dark period. Notably, incorporation into the lipid fraction was low at all treatments.

For the high photon irradiance, the amounts of water-extractable mono- and polysaccharides in the particulate fraction were measured at the beginning and end of the light period (Figure 4). The mean amounts per unit of Chl *a* were significantly different between the morning and the afternoon at a 95% confidence level (two-factor

Table II: The average diurnal carbon incorporation rates [in μg C (μg Chl a)$^{-1}$ h^{-1}] into several fractions (glucan, proteins and total) at low (LL) and high (HL) photon irradiance for the geographic regions APF, ACC and MIZ

	APF (n = 5)		ACC (n = 2)		MIZ (n = 1)	
	Control	+Fe	Control	+Fe	Control	+Fe
LL						
Glucan	0.16 (0.04)	0.16 (0.02)	0.16 (0.05)	0.13 (0.05)	0.16	0.21
Proteins	0.14 (0.01)	0.15 (0.02)	0.16 (0.04)	0.16 (0.02)	0.20	0.20
Total	0.48 (0.07)	0.49 (0.04)	0.49 (0.12)	0.44 (0.13)	0.59	0.64
HL						
Glucan	0.94 (0.17)	0.95 (0.12)	0.91 (0.05)	0.88 (0.16)	0.90	1.02
Proteins	0.21 (0.01)	0.21 (0.02)	0.23 (0.07)	0.25 (0.03)	0.27	0.35
Total	1.57 (0.23)	1.57 (0.19)	1.60 (0.15)	1.57 (0.26)	1.66	1.95

See Table I for abbreviations. The rates are presented for control and iron amended bottles separately. Standard deviations are between brackets.

ANOVAs with iron level and time of day as factors). The diurnal increase in polysaccharides, that probably mostly consist of storage carbohydrates, was more pronounced than the increase in monosaccharides. Consequently, the ratio of poly- to monosaccharides increased from 1.4 to 1.8 during the day. There was no significant effect of iron addition on the carbohydrate concentration. The diurnal increase in the amount of carbohydrates was mainly caused by an increase in glucose (Figure 5); the amounts of other neutral aldoses were lower and hardly increased. The contribution of glucose to the total amount of neutral aldoses increased during the light period from 46 to 63%. Its relative contribution was again not significantly dependent on iron.

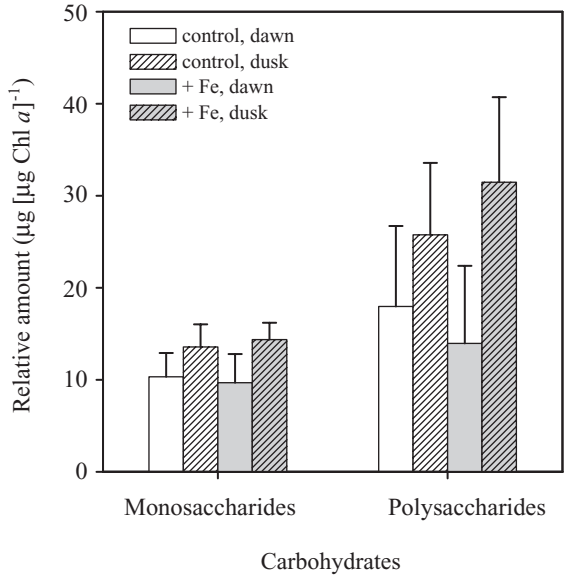

Fig. 4. The Chl *a*-specific amount of water-extractable mono- and polysaccharides at the start and the end of the light period for natural phytoplankton communities of the APF (exp. no 1, 2, 7 and 8) incubated with and without addition of iron. Error bars indicate standard deviations (n = 4).

Comparison with ACC and MIZ

The average diurnal carbon assimilation per litre of seawater at the APF was 7400 and 2200 μg C, at high and low photon irradiance, respectively. In agreement with the lower Chl *a* biomass encountered, the carbon assimilation in the ACC and the MIZ were, respectively, 2- and 4-fold lower, at both light intensities. The Chl *a*-specific rates of carbon incorporation were similar for all regions at both light intensities (Table II). Furthermore, the patterns of incorporation were the same (in Table II glucan and proteins are presented) and for the APF and the ACC no effect of iron addition was evident. For the MIZ, the carbon incorporation was highest in the iron enriched bottles, but this does not warrant much interpretation since only one experiment was performed. When all experiments were combined, a strong correlation between the total diurnal C incorporation and the Chl *a* concentration was found at both light intensities (Pearson product moment correlations, HL: r = 0.96, n = 8; LL: r = 0.96, n = 8). The correlation between glucan-C incorporation and Chl *a* was also strong (HL: r = 0.97, n = 8; LL: r = 0.95, n = 8).

The Chl *a*-specific water-extractable amount of polysaccharides measured by chemical analysis was similar for APF and ACC samples: 16 versus 18 μg μg^{-1}, respectively, in the morning; 28 versus 32 μg μg^{-1} in the afternoon and no significant effect of iron addition. The neutral aldose composition of the water-extractable carbohydrates (GC analysis) in ACC samples was also

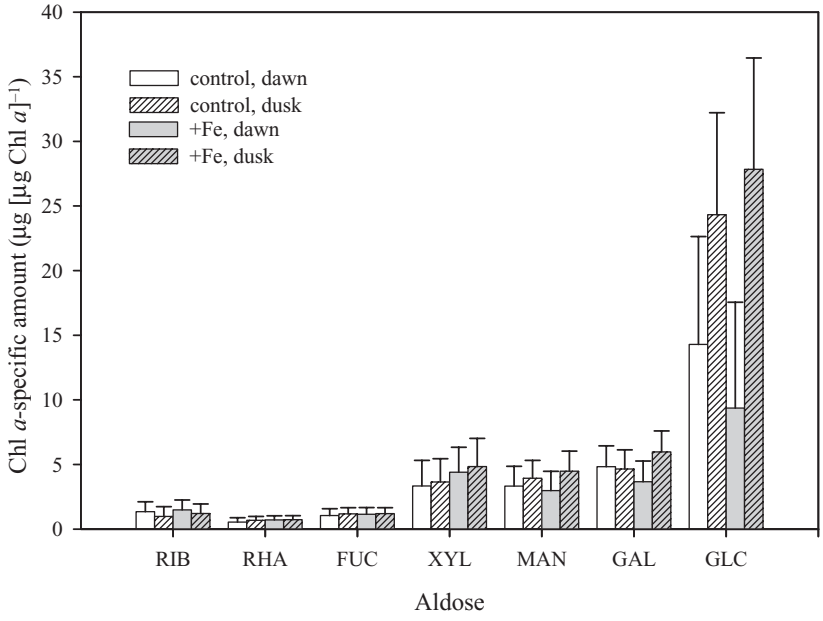

Fig. 5. The Chl *a*-specific amount of aldoses at the start and the end of the light period in experiments with natural phytoplankton communities of the APF (exp. no 1, 2, 7 and 8) incubated with and without addition of iron. Error bars indicate standard deviations ($n = 4$). RIB, ribose; RHA, rhamnose; FUC, fucose; XYL, xylose; MAN, mannose; GAL, galactose; GLC, glucose.

similar to that in APF samples: glucose contributed 47% in the morning and 63% in the afternoon. For the MIZ experiment, no samples were taken for chemical analysis of carbohydrates.

Laboratory experiment

In Figure 6 the patterns of ^{14}C assimilation into the different biochemical pools are presented for a laboratory experiment with cultures of *C. brevis*. During long-term incubations (filled circles), 43% of the newly assimilated carbon was incorporated into glucan at the end of the light period and 7% into amino acids; 30% was incorporated into proteins, 18% into polysaccharides and lipids contributed only 2%. The contributions of glucan and amino acids fractions were relatively low compared with contributions in the natural phytoplankton populations that were kept at the comparable irradiance (Figure 3, HL, open circles). The amount of carbon incorporated into the glucan fraction decreased strongly during the dark period (Figure 6A), stronger than during the experiments with the natural populations (Figure 3A). As observed for the natural populations, protein synthesis continued during the dark period and lipid synthesis stopped (Figure 6C,D). For the amino acids fraction, the plot of carbon incorporation versus time exhibited a strong downward concavity over the light period for the long-term incubations but not so for the cumulative short-term incubations (Figure 6B). The estimated diurnal rate of carbon incorporation was significantly higher if based on the latter type of incubations, 28 versus 17 fg C cell^{-1} h^{-1} (one-way ANOVA, $P < 0.05$). In contrast, for the proteins fraction the estimate was significantly lower, 55 versus 73 fg C cell^{-1} h^{-1} (one-way ANOVA, $P < 0.05$) (Figure 6C). For the glucan, lipid and protein fractions there were only minor differences in the estimated diurnal carbon incorporation based on long-term or cumulative short-term incubations.

As observed for the ^{14}C incorporation into the glucan fraction, the water-extractable polysaccharide concentration in the particulate fraction determined by chemical analysis (TPTZ method) showed a diel pattern (Figure 7). This pattern was more clearly visible in the cellular polysaccharide content than in the monosaccharide content. Hence, the ratio of polysaccharides to monosaccharides increased from 3.2 to 6.6 over the light period.

DISCUSSION

It is clear that the populations we encountered in the Southern Ocean were not predominantly iron-limited during austral Autumn. The fact that patterns of photosynthate allocation did not change after iron addition does in itself not exclude iron limitation. Van Leeuwe *et al.* (Van Leeuwe *et al.*, 1997) did not observe a change in these patterns either, despite a clear iron response in POC and Chl *a* synthesis and in the consumption of major nutrients. Apparently, the Antarctic phytoplankton studied by these authors in austral summer endured low iron

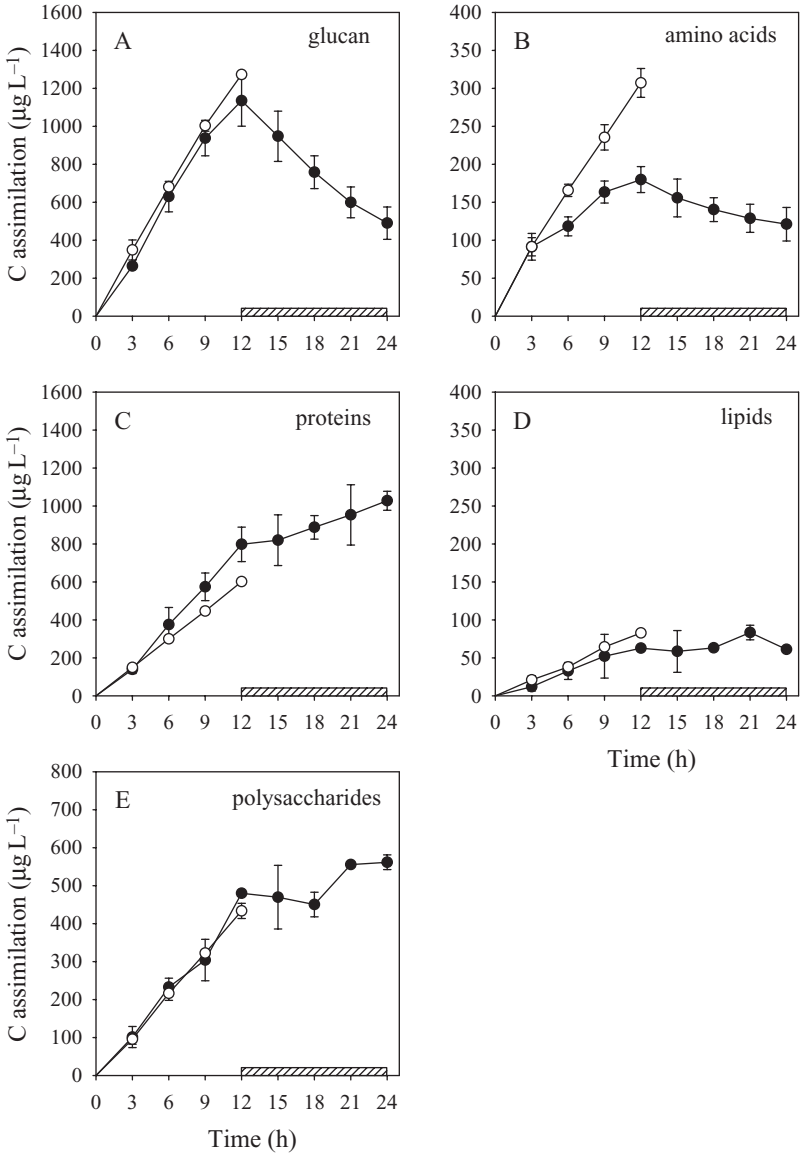

Fig. 6. The carbon assimilation into the biochemical pools (**A**) glucan, (**B**) amino acids, (**C**) proteins, (**D**) lipids and (**E**) polysaccharides estimated by long-term (24 h) and cumulative short-term (3 h) ^{14}C incubations with the Antarctic diatom *Chaetoceros brevis*. Error bars indicate standard deviations (n = 2), in some cases deviations are smaller than symbols. Filled circles are long-term, open circles are cumulative short-term. The dashed bars indicate the dark periods.

concentrations by maintaining physiological processes at low activity rates. However, in contrast to their study made in austral summer, iron addition did not result in an increase in the rates of total carbon assimilation and carbohydrate production. Furthermore, for all field measurements made during our cruise the correlation between Chl *a* and iron concentrations was weak, much weaker than observed during summer (Croot and De Jong, 2000).

Altogether, this suggests that another factor was limiting phytoplankton growth at this time of year and caused the differences in phytoplankton abundance between regions. Light availability is a likely candidate. The light climate was no doubt unfavourable for phytoplankton growth because the incident irradiance was low during the time of the cruise: irradiance varied between no more than 2–10 MJ m^{-2} day^{-1} at the sea surface. Furthermore, the mixed layer was deep, 50–100+ m due to high wind speeds and frequent storms (Strass and Leach, 2000). We observed that phytoplankton production was strongly light-limited at a photon irradiance of 20 μmol photons m^{-2} s^{-1}, which corresponds to the average irradiance at 20–45 m depth [based on

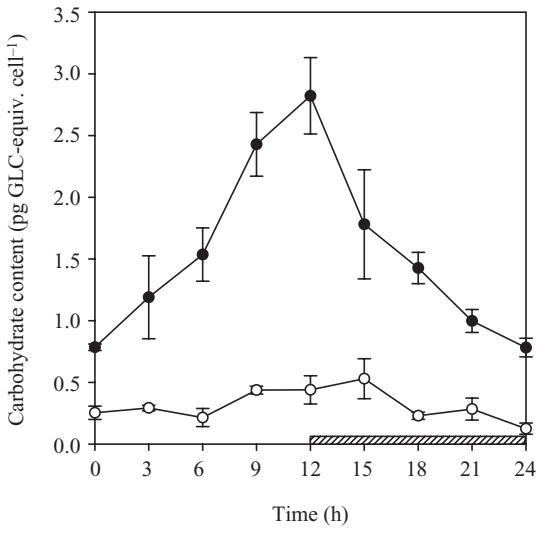

Fig. 7. The diel change in the cellular water-extractable monosaccharide (open circles) and polysaccharide (filled circles) content in the particulate fraction during a 24 h incubation experiment with *C. brevis*. The dashed bar indicates the dark period.

an extinction coefficient of 0.06, see Van Oijen *et al.* (Van Oijen *et al.*, 2003)].

During the time of the cruise, there was a distinct difference in mixing depth between regions. At the APF this depth was 50–60 m whereas in the ACC the mixing was sometimes in excess of 100 m (Strass and Leach, 2000). This difference could not only explain the observed variations in phytoplankton abundance but also the variations in species composition. In a study in the Ross Sea, diatoms dominated in stratified waters and were less abundant where waters were mixed more deeply (Arrigo *et al.*, 1999). The diatoms were less capable of maintaining near-maximal photosynthetic rates at low irradiance levels than *Phaeocystis antarctica*. Indeed, during our cruise flagellates dominated the more turbulent waters of the ACC. However, we did not find a significant difference in the Chl *a*-normalized carbon assimilation rate between regions at the photon flux densities tested.

As an alternative, we suggest that the abundance of small phytoplankton was controlled by microzooplankton grazing in all regions whereas the grazing pressure on the sturdy diatoms (Hamm *et al.*, 2003) was lower, so they became dominant where light conditions were sufficient to sustain enhanced growth rates. We do not have data to support this, but the role of differential grazing pressure has been emphasized previously for other High Nitrate Low Chlorophyll (HNLC) regions by Cullen (Cullen, 1991) and Banse (Banse, 1996).

The low seawater temperatures may have set an upper limit to phytoplankton growth rates (Tilzer *et al.*, 1986; Reay *et al.*, 2001), but they alone cannot explain the low biomass encountered since high Chl *a*-specific rates of carbon incorporation were measured at ambient temperature and high irradiance. Limitations by major nutrients are unlikely in the ACC because nutrients were available at growth-saturating concentrations. Silicic acid concentrations were in fact lower at the APF, which may well be due to the high diatom abundance.

Although we can confidently state that the resident populations were not iron-limited at the photon flux densities that we used in our experiments, we cannot exclude the possibility that *in situ* phytoplankton production was co-limited by light and iron. At low photon flux densities, iron requirements are much higher (Raven, 1990; Sunda and Huntsman, 1997). In the Pacific, Maldonado *et al.* (Maldonado *et al.*, 1999) observed a strong increase in carbon fixation 24 h after iron addition when field communities were exposed to very low photon flux densities of 0.27–1.09 mol quanta m^{-2} day^{-1}. However, at an irradiance comparable with the one we applied, they did not observe a response to iron addition. If we extrapolate those results to the conditions during our cruise, co-limitation of iron and light is likely in regions where mixing is deep. Hence, the shallower mixing depth and concomitant increase in light availability at the APF may have decreased the iron requirement of phytoplankton, which would facilitate enhanced growth rates.

In addition, phytoplankton species that contributed little to the total cell numbers, e.g. diatoms in the ACC, may have been limited to some extent by iron availability. In other words a response to the iron addition of these species may not have been detectable in the overall community response during our experiments, which were short-term (48 h). Evidence that large diatoms can be iron-limited in the ACC has been provided by Timmermans *et al.* (Timmermans *et al.*, 2001) who, during the same cruise, incubated monocultures of the diatom *Chaetoceros dichaeta* (>20 μm) in filtered natural seawater under the same irradiance. They estimated a half-saturation constant (K_m) for growth of 1.12 nM of dissolved iron, implying that this species is iron-limited at the ambient concentrations of the ACC. In contrast, a smaller diatom species, *C. brevis*, had a very low K_m value, and thus a high affinity for iron so it was probably not iron-limited. This low iron requirement is in keeping with its high surface-to-volume ratio which is beneficial for iron uptake (Hudson and Morel, 1990).

Consistency between ^{14}C incorporation in field and laboratory experiments

The fractionation method developed by Granum and Myklestad (Granum and Myklestad, 2001) was used for the first time on field samples and over a 24 h period.

The method distinguishes biochemical pools with their own characteristic behaviours that illustrate the sequential steps of carbon incorporation. During the first three hours of the light period, carbon incorporation in amino acids was high. The strong downward curvature of the plot of the diurnal incorporation of ^{14}C into amino acids (Figure 6B) indicates a high turnover rate of these molecules that are needed as precursors for protein synthesis. The incorporation of labelled carbon into proteins was probably initially low (Figure 6C) due to the time it takes to synthesize amino acids. Over the remaining light period, the carbon incorporation into proteins showed a continuous rise, indicating a low consumption. The glucan pool showed a diel pattern with high production during the light period but a decrease during the dark period. This is consistent with its suggested role as a diel reserve supplying energy and carbon skeletons for continued protein synthesis at night (Cuhel *et al.*, 1984). Indeed, carbon incorporation into proteins proceeded at night albeit at a lower rate. Our field experiments showed that at low photon irradiance, the diurnal production of glucan was strongly decreased, much more than the production of any other pool. Probably at low irradiance the incorporated carbon was used directly for the synthesis of proteins and other metabolites and not accumulated in the form of glucan. In agreement, there was a relatively small difference in the diurnal rate of protein synthesis between the two photon flux densities.

To gain more insight into the dynamics of the glucan pool, we constructed a simple model to predict the glucan production and respiration during the light and dark period (Table III, see Appendix for details). The model fits to the ^{14}C data were in good agreement with the dynamics in the total water-extractable carbohydrate concentration determined by chemical analysis, especially for the culture experiment with *C. brevis* (Figure 8). The diurnal cellular glucan production rate (P_d) was highest for cells of the natural populations. This difference was likely related to the difference in cell volume, which was approximately 50 μm^3 for *C. brevis* and over 30 times higher for the field communities. The diurnal glucan consumption rate (R_d) was estimated to be 30–40% of the production rate for both the experiment with *C. brevis* and the field experiments (Table III). The cellular nocturnal respiration rate (R_n) of glucan was 1.5–2.7 higher than the diurnal respiration rate (R_d). In contrast, using a different model and a different fractionation procedure, Lancelot and Mathot (Lancelot and Mathot, 1985) estimated higher rates of glucan respiration during the day than at night for a mixed diatom population in Belgian coastal waters. Another study found no difference in respiration between day and night (Foy and Smith, 1980). More research is needed to resolve these differences.

When comparing the strong decrease in radioactivity in the glucan fraction during the dark period in the *C. brevis* cultures with the more modest decrease in radioactivity in the field experiments (Figures 3A and 6A), one might wonder why the relative proportions of the modelled diurnal and nocturnal respiration rate (R_d and R_n) and the

Table III: Parameter values for model used to fit data for the laboratory experiments with C. brevis and shipboard experiments with natural field communities of the APF

Parameter	Culture *C. brevis* (n = 2)	Field community APF (n = 4)	
		LL	HL
Input			
^{14}C carbonate activity (MBq L^{-1})	0.40 (0.02)	7.45 (1.45)	7.45 (1.45)
C_{med} (mg C L^{-1})	19.5 (0.04)	25.8 (0.11)	25.8 (0.11)
Cell number (mL^{-1})	768 000 (3 000)	350 (75)	350 (75)
C_0 (pg C $cell^{-1}$)	0.42 (0.02)	12.8 (1.40)	12.8 (1.40)
μ (day^{-1})	0.45 (0.01)	0.075[a]	0.30[a]
Output[b]			
P_d (fg C $cell^{-1}$ h^{-1})	247 (35)	408 (67)	2450 (483)
R_d (fg C $cell^{-1}$ h^{-1})	98 (20)	108 (208)	892 (617)
R_n (fg C $cell^{-1}$ h^{-1})	148 (15)	300 (208)	1558 (317)

Standard deviations are between brackets. For abbreviations, see Appendix.

[a]The growth rate applied to fit the model to the field data was based on two 6 day experiments under similar experimental conditions, during which cells were counted with a flow cytometer every 2 days (Van Leeuwe and Van Oijen, 2000).

[b]The model was fitted to the ^{14}C data using the equation editor of Sigmaplot 8.0. The fit was constrained by the values measured for the listed input parameters.

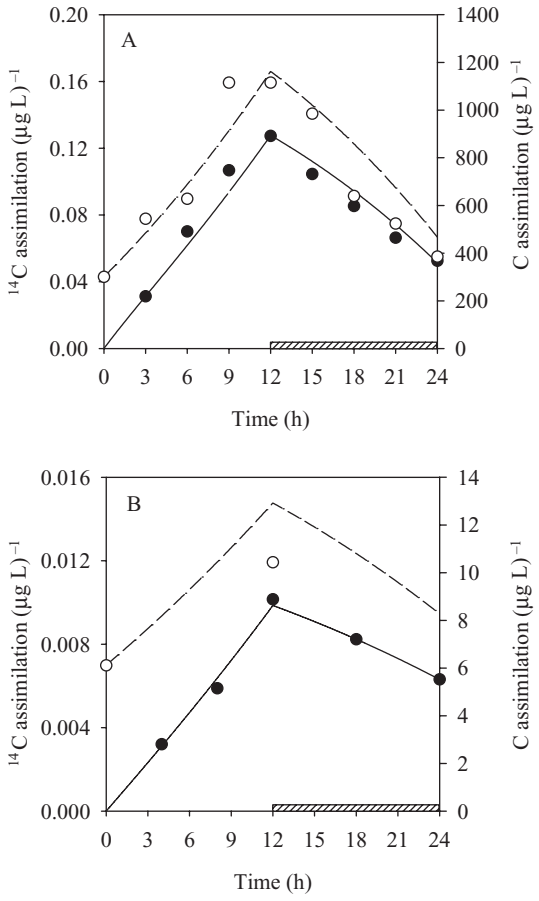

Fig. 8. Comparison between model predictions and measured data of ^{14}C carbon assimilation into glucan (closed symbols are data, solid line is model fit) and the total water-extractable carbohydrate concentration in the particulate fraction (open symbols are data, dashed line is model fit) for (**A**) the culture experiment with *C. brevis* and (**B**) a field experiment with a natural phytoplankton community of the APF. The dashed bars indicate the dark period.

diurnal glucan production (P_d) are so similar for the field populations and the *C. brevis* cultures. However, a difference in the decrease in radioactivity does not imply that the respiration rate is different because the losses in radioactivity are proportional to R_d multiplied by ^{14}C/C [see Appendix, equation (5)]. Since C is partly determined by the initial cellular amount of unlabelled carbohydrates (C_0) and C_0 was much higher for cells of the natural phytoplankton populations, only a small proportion of the total glucan-C pool was labelled in these populations at the end of the light period. Therefore, much unlabelled carbon was respired relative to ^{14}C. The initial pool size was probably related to the cell volume.

Notably, the contribution of the glucan and amino acids fractions to the total ^{14}C incorporation was relatively high in the field experiments compared with the experiment with *C. brevis*. This is consistent with the suggestion of Thomas and Gleitz (Thomas and Gleitz, 1993) that large, slowly growing diatom species incorporate high amounts of carbon into low molecular weight metabolites whereas small, fast growing species are characterized by a high carbon turnover associated with a rapid flow of newly assimilated carbon into polymeric compound classes.

The ^{14}C fractionation method we have used here can be further improved by separation of the storage polysaccharides and the monosaccharides by size fractionation. Especially monosaccharides play an important role in the regulation of the osmotic pressure in plant cells (Dickson and Kirst, 1987a, b). Indeed, the cellular monosaccharide content remained more or less constant throughout the day (Figures 4 and 7) and the ratio of monosaccharides to polysaccharides was much higher in the small *C. brevis* cells than in the field samples. The model could be further developed to include these two pools. In addition, especially at high irradiance, part of the diurnal loss of water-extractable carbohydrates may not be related to respiration but to extracellular release of carbohydrates as an overflow mechanism. The model should be adjusted to differentiate between these loss processes. A further improvement of the model could be to include synchronized cell division if observed. This requires more data on changes in cell number during the course of the experiment. A lack of these data was the main source of uncertainty in the model output for the field experiments.

CONCLUSION

Our study indicates that the resident phytoplankton in the Southern Ocean during austral Autumn is controlled by the low light rather than by iron limitation. The higher production and domination by diatoms at the Antarctic Polar Front can be explained by a more favourable light climate due to the relatively high vertical stability of the water column that we encountered, possibly in combination with differential grazing pressure on the various size classes in the phytoplankton. Especially in the Antarctic Circumpolar Current diatoms could be co-limited by iron and light, but direct evidence for this dual control cannot be presented here. The diurnal carbohydrate production was highest at the Antarctic Polar Front, which may have influenced other components of the ecosystem. Indeed, not only production of storage carbohydrates (in diatoms mainly consisting of glucose) can be higher but also the production of complex exopolysaccharides that are known to contribute to the water-extractable carbohydrate fraction [Hama and Handa (Hama and Handa, 1992) and Figure 5]. A considerable part of these carbohydrates is usually excreted and ends up in the water column to

become a carbon source for bacteria (Benner *et al.*, 1992; Pakulski and Benner, 1994; Biddanda and Benner, 1997; Hama and Yanagi, 2001). Hence, if carbohydrate production in a certain region is affected, this may have consequences for the microbial food web. In fact, the highest heterotrophic acitivity was documented at the APF during the same cruise (Simon *et al.*, 2000). The next step in our study programme would be to explore this link.

ACKNOWLEDGEMENTS

We thank captain and crew of R.V. Polarstern for their support during deck operations, G. Kattner and colleagues for nutrient analysis, S. Kirkvold for TCO_2 analysis in cultures, J. de Jong for iron analysis and V. Schoemann, K. Timmermans and P. Croot for general assistance. We are grateful to Prof. S. Myklestad for advice and providing the opportunity of a three month research period at the Dept of Biotechnology of the Norwegian University of Science & Technology in Trondheim, Norway. This research was supported by the European Commission's Environmental and Climate Research programme CARUSO (CARbon dioxide Uptake by the Southern Ocean, EC contract no ENV4-CT 97–0472). Additional financial support was provided by a Marie Curie Fellowship of the European Community programme 'Improving Human Research Potential and the socio-economic Knowledge Base' under contract no HPMT-CT-2001–00424.

REFERENCES

Arar, E. J. and Collins, G. B. (1992) Method 445.0 – in vitro determination of Chl *a* and phaeophytin *a* in marine and freshwater phytoplankton by fluorescence. In *US EPA Methods for the Determination of Chemical Substances in Marine and Estuarine Environmental Samples*. U.S. Environmental Protection Agency, Cincinnati, pp. 1–14.

Arrigo, K. R., Robinson, D. H., Worthen, D. L., Dunbar, R. B., Ditullio, G. R., Vanwoert, M. and Lizotte, M. P. (1999) Phytoplankton community structure and the drawdown of nutrients and CO_2 in the Southern Ocean. *Science*, **283**, 365–367.

Banse, K. (1996) Low seasonality of low concentrations of surface chlorophyll in the Subantarctic water ring: underwater irradiance, iron or grazing? *Progr. Oceanog.*, **37**, 241–291.

Barber, R. T. (2002) SOFeX: Southern Ocean iron experiments. An overview of the biological responses. *Eos Trans. AGU*, **83**, Fall Meet. Suppl., Abstract OS22D-02.

Behrenfeld, M. J., Bale, A. J., Kolber, Z. S., Aiken, J. and Falkowski, P. G. (1996) Confirmation of iron limitation of phytoplankton photosynthesis in the equatorial Pacific Ocean. *Nature*, **383**, 508–511.

Benner, R., Pakulski, J. D., McCarthy, M., Hedges, J. I. and Hatcher, P. G. (1992) Bulk chemical characteristics of dissolved organic matter in the ocean. *Science*, **255**, 1561–1564.

Biddanda, B. and Benner, R. (1997) Carbon, nitrogen, and carbohydrate fluxes during the production of particulate and dissolved organic matter by marine phytoplankton. *Limnol. Oceanogr.*, **42**, 506–518.

Boyd, P. W. (2002) Environmental factors controlling phytoplankton processes in the Southern Ocean. *J. Phycol.*, **38**, 844–861.

Boyd, P. W. and Abraham, E. R. (2001) Iron-mediated changes in phytoplankton photosynthetic competence during SOIREE. *Deep-Sea Res. II*, **48**, 2529–2550.

Boyd, P. W., Watson, A. J., Law, C. S. *et al.* (2000) A mesoscale phytoplankton bloom in the polar Southern Ocean stimulated by iron fertilization. *Nature*, **407**, 695–702.

Bracher, A. U., Kroon, B. M. A. and Lucas, M. I. (1999) Primary production, physiological state and composition of phytoplankton in the Atlantic Sector of the Southern Ocean. *Mar. Ecol. Prog. Ser.*, **190**, 1–16.

Croot, P. L. and De Jong, J. T. M. (2000) Field distribution of iron in a section of the Antarctic Polar Frontal Zone. *Ber. Polarforsch. Meeresforsch.*, **364**, 44–47.

Cuhel, R. L., Ortner, P. B. and Lean, D. R. S. (1984) Night synthesis of protein by algae. *Limnol. Oceanogr.*, **29**, 731–744.

Cullen, J. J. (1991) Hypotheses to explain high-nutrient conditions in the open sea. *Limnol. Oceanogr.*, **36**, 1578–99.

Davey, M. S. and Geider, R. J. (2001) Impact of iron limitation on the photosynthetic apparatus of the diatom *Chaetoceros muelleri* (Baccillariophyceae). *J. Phycol.*, **37**, 987–1000.

De Baar, H. J. W. and Boyd, P. W. (2000) The role of iron in plankton ecology and carbon dioxide transfer of the global oceans. In Hanson, R. B., Ducklow, H. W. and Field, J. G. (eds), *The Changing Ocean Carbon Cycle*. Cambridge University Press, Cambridge, pp. 61–140.

De Baar, H. J. W. and De Jong, J. T. M. (2001) Distributions, sources and sinks of iron in seawater. In Turner, D. R. and Hunter, K. A. (eds), *The Biogeochemistry of Iron in Seawater*. John Wiley & Sons, Chichester, pp. 123–253.

De Baar, H. J. W., De Jong, J. T. M., Bakker, D. C. E., Löscher, B. M., Veth, C., Bathmann, U. and Smetacek, V. (1995) Importance of iron for plankton blooms and carbon dioxide drawdown in the Southern Ocean. *Nature*, **373**, 412–415.

De Jong, J. T. M., Den Das, J., Bathmann, U., Stoll, M. H. C., Kattner, G., Nolting, R. F. and De Baar, H. J. W. (1998) Dissolved iron at subnanomolar levels in the Southern Ocean as determined by ship-board analysis. *Anal. Chim. Acta*, **377**, 113–124.

Dickson, D. M. J. and Kirst, G. O. (1987a) Osmotic adjustment in marine eukaryotic algae: the role of inorganic ions, quaternary ammonium, tertiary sulphonium and carbohydrate solutes. I. Diatoms and a Rhodophyte. *New Phytol.*, **106**, 645–655.

Dickson, D. M. J. and Kirst, G. O. (1987b) Osmotic adjustment in marine eukaryotic algae: the role of inorganic ions, quaternary ammonium, tertiary sulphonium and carbohydrate solutes. II. Prasinophytes and Haptophytes. *New Phytol.*, **106**, 657–666.

DOE (1994) *Handbook of Methods for the Analysis of the Various Parameters of the Carbon Dioxide System in Sea Water; version 2*. ORNL/CDIAC-74.

Dring, M. J. and Jewson, D. H. (1982) What does ^{14}C uptake by phytoplankton really measure? A theoretical modelling approach. *Proc. R. Soc. Lond. B*, **214**, 351–368.

Edelstein-Keshet, L. (1988) *Mathematical Models in Biology*. Random House, New York.

Falkowski, P. G., Barber, R. T. and Smetacek, V. (1998) Biogeochemical controls and feedbacks on ocean primary production. *Science*, **281**, 200–206.

Foy, R. H. and Smith, R. V. (1980) The role of carbohydrate accumulation in the growth of planktonic *Oscillatoria* species. *Br. Phycol. J.*, **15**, 139–150.

Franck, M., Brzezinski, M. A., Coale, K. H. and Nelson, D. M. (2000) Iron and silicic acid concentrations regulate Si uptake north and south of the Polar Frontal Zone in the Pacific Sector of the Southern Ocean. *Deep-Sea Res. II*, **47**, 3315–3338.

Geider, R. J. and La Roche, J. (1994) The role of iron in phytoplankton photosynthesis and the potential for iron-limitation of primary productivity in the sea. *Photosynth. Res.*, **39**, 275–301.

Geider, R. J. and Osborne, B. A. (1992) Using isotopes to measure gas exchange. In Geider, R. J. and Osborne, B. A. (eds), *Algal Photosynthesis*. Chapman and Hall, New York, pp. 32–70.

Gervais, F., Riebesell, U. and Gorbunov, M. Y. (2002) Changes in size-fractionated primary productivity and chlorophyll *a* in response to iron fertilization in the Southern Polar Frontal Zone. *Limnol. Oceanogr.*, **47**, 1324–1335.

Granum, E. and Myklestad, S. M. (1999) Effects of NH_4^+ assimilation on dark carbon fixation and b-1,3-glucan metabolism in the marine diatom *Skeletonema costatum* (Bacillariophyceae). *J. Phycol.*, **35**, 1191–1199.

Granum, E. and Myklestad, S. M. (2001) Mobilization of beta-1,3-glucan and biosynthesis of amino acids induced by NH_4^+ addition to N-limited cells of the marine diatom *Skeletonema costatum* (Bacillariophyceae). *J. Phycol.*, **37**, 772–782.

Guillard, R. R. L. (1975) Culture of phytoplankton for feeding marine invertebrates. In Smith, W. L. and Chanley, M. H. (eds), *Culture of Marine Invertebrate Animals*. Plenum Press, New York, pp. 26–60.

Hama, J. and Handa, N. (1992) Diel variation of water-extractable carbohydrate composition of natural phytoplankton populations in Kinu-ura Bay. *J. Exp. Mar. Biol. Ecol.*, **162**, 159–176.

Hama, T. and Yanagi, K. (2001) Production and neutral aldose composition of dissolved carbohydrates excreted by natural marine phytoplankton populations. *Limnol. Oceanogr.*, **46**, 1945–1955.

Hamm, C. E., Merkel, R., Springers, O., Jurkojc, P., Maier, C., Prechtel, C. and Smetacek, V. (2003) Architecture and material properties of diatom shells provide effective mechanical protection. *Nature*, **421**, 841–843.

Hartmann, C., Kattner, G. and Ratje, A. (2000) Distribution of nutrients. *Ber. Polarforsch. Meeresforsch.*, **364**, 38–42.

Hitchcock, G. L. (1980) Diel variation in chlorophyll *a*, carbohydrate and protein content of the marine diatom *Skeletonema costatum*. *Mar. Biol.*, **57**, 271–278.

Hudson, R. J. M. and Morel, F. M. M. (1990) Iron transport in marine phytoplankton: kinetics of cellular and medium coordination reactions. *Limnol. Oceanogr.*, **35**, 1002–1020.

Hutchins, D. A., Sedwick, P. N., DiTullio, G. R., Boyd, P. W., Queguiner, B., Griffiths, F. B. and Crossley, C. (2001) Control of phytoplankton growth by iron and silicic acid availability in the subantarctic Southern Ocean: experimental results from the SAZ project. *J. Geophys. Res. C: Oceans*, **106**, 31559–31572.

Jacques, G. (1989) Primary production in the open Antarctic ocean during austral summer. A review. *Vie Milieu*, **39**, 1–17.

Johnson, K. M., Sieburth, J. M., Williams, P. J. l. B. and Brandström, L. (1987) Coulometric total carbon dioxide analysis for marine studies: automation and calibration. *Mar. Chem.*, **21**, 117–133.

Kamerling, J. P. and Vliegenthart, J. F. G. (1989) Carbohydrates. In Lawson, A. M. (ed.), *Mass Spectrometry*. de Gruyter, New York, pp. 177–263.

Koeman, R. P. T. (1999) Analyses van fytoplankton en microzoöplankton van het Friese Front 1999. Rapportage van onderzoek in opdracht van het Rijksinstituut voor Kust en Zee (RIKZ). In Dutch.

Kolber, Z. S., Barber, R. T., Coale, K. H., Fitzwater, S. E., Greene, R. M., Johnson, K. S., Lindley, S. and Falkowski, P. G. (1994) Iron limitation of phytoplankton photosynthesis in the equatorial Pacific Ocean. *Nature*, **371**, 145–149.

Lancelot, C. and Mathot, S. (1985) Biochemical fractionation of primary production by phytoplankton in Belgian coastal waters during short- and long-term incubations with ^{14}C-bicarbonate. I. Mixed diatom population. *Mar. Biol.*, **86**, 219–226.

Lancelot, C., Hannon, E., Becquevort, S., Veth, C. and De Baar, H. J. W. (2000) Modeling phytoplankton blooms and carbon export production in the Southern Ocean: dominant controls by light and iron in the Atlantic sector in Austral spring 1992. *Deep-Sea Res. I*, **47**, 1621–1662.

Laubscher, R. K., Perissinotto, R. and McQuaid, C. D. (1993) Phytoplankton production and biomass at frontal zones in the Atlantic sector of the Southern Ocean. *Polar Biol.*, **13**, 471–481.

Li, W. K. W., Glover, H. E. and Morris, I. (1980) Physiology of carbon photoassimilation by *Oscillatoria thiebautii* in the Caribbean Sea. *Limnol. Oceanogr.*, **25**, 447–456.

Lutjeharms, J. R. E., Walters, N. M. and Allanson, B. R. (1985) Oceanic frontal systems and biological enhancement. In Siegfried, W. R., Condy, P. R. and Laws, R. M. (eds), *Antarctic Nutrient Cycles and Food Webs*. Springer-Verlag, Berlin, pp. 11–22.

Maldonado, M. T., Boyd, P. W., Harrison, P. J. and Price, N. M. (1999) Co-limitation of phytoplankton growth by light and Fe during winter in the NE subarctic Pacific Ocean. *Deep-Sea Res. II*, **46**, 2475–2485.

Morris, I., Glover, H. E. and Yentsch, C. S. (1974) Products of photosynthesis by marine phytoplankton: the effect of environmental factors on the relative rates of protein synthesis. *Mar. Biol.*, **27**, 1–9.

Myklestad, S. M., Skånøy, E. and Hestmann, S. (1997) A sensitive and rapid method for analysis of dissolved mono- and polysaccharides in seawater. *Mar. Chem.*, **56**, 279–286.

Nelson, D. M., Brzezinski, M. A., Sigmon, D. E. and Franck, V. M. (2001) A seasonal progression of Si limitation in the Pacific sector of the Southern Ocean. *Deep-Sea Res. II*, **48**, 3973–3995.

Pakulski, J. D. and Benner, R. (1994) Abundance and distribution of carbohydrates in the ocean. *Limnol. Oceanogr.*, **39**, 930–940.

Raven, J. A. (1990) Predictions of Mn and Fe use efficiencies of phototrophic growth as a function of light availability for growth and of C assimilation pathway. *New Phytol.*, **116**, 1–18.

Reay, D. S., Priddle, J., Nedwell, D. B., Whitehouse, M. J., Ellis-Evans, J. C., Deubert, C. and Connelly, D. P. (2001) Regulation by low temperature of phytoplankton growth and nutrient uptake in the Southern Ocean. *Mar. Ecol. Prog. Ser.*, **219**, 51–64.

Robinson, C. and Williams, P. J. l. B. (1992) Development and assessment of an analytical system for the accurate and continual measurement of total dissolved inorganic carbon. *Mar. Chem.*, **34**, 157–175.

Simon, M., Rosenstock, B. and Zwisler, W. (2000) Biomass production, substrate dynamics and community structure of the heterotrophic picoplankton at the polar front and the Weddell Sea in fall. *Ber. Polarforsch. Meeresforsch.*, **364**, 91–100.

Smetacek, V. (2000) The giant diatom dump. *Nature*, **406**, 574–575.

Stoll, M. H. C. (1994) *Inorganic Carbon Behaviour in the North Atlantic Ocean*. Phd Thesis. University of Groningen, Groningen, The Netherlands. ISBN 90–9007535–6.

Strass, V. and Leach, H. (2000) Physical control of primary production and of biogeochemical fluxes at the Antarctic Polar Front. *Ber. Polarforsch. Meeresforsch.*, **364**, 16–37.

Sunda, W. G. and Huntsman, S. A. (1997) Interrelated influence of iron, light and cell size on marine phytoplankton growth. *Nature*, **390**, 389–392.

Thomas, D. N. and Gleitz, M. (1993) Allocation of photoassimilated carbon into major algal metabolite fractions: variation between two diatom species isolated from the Weddell Sea (Antarctica). *Polar Biol.*, **13**, 281–286.

Tilzer, M. M., von Bodungen, B. and Smetacek, V. (1985) Light-dependence of phytoplankton photosynthesis in the Antarctic Ocean: implications for regulating productivity. In Siegfried, W. R., Condy, P. R. and Laws, R. M. (eds), *Antarctic Nutrient Cycles and Food Webs*. Springer-Verlag, Berlin, pp. 60–69.

Tilzer, M. M., Elbrächter, M., Gieskes, W. W. C. and Beese, B. (1986) Light-temperature interactions in the control of photosynthesis in Antarctic phytoplankton. *Polar Biol.*, **5**, 105–111.

Timmermans, K. R., Gerringa, L. J. A., De Baar, H. J. W., Van der Wagt, B., Veldhuis, M. J. W., De Jong, J. T. M., Croot, P. L. and Boye, M. (2001) Growth rates of large and small Southern Ocean diatoms in relation to availability of iron in natural seawater. *Limnol. Oceanogr.*, **46**, 260–266.

Van Leeuwe, M. A. and Van Oijen, T. (2000) Light adaptation by natural phytoplankton populations, and its control by iron limitation. *Ber. Polarforsch. Meeresforsch.*, **364**, 77–83.

Van Leeuwe, M. A., Scharek, R., De Baar, H. J. W., De Jong, J. T. M. and Goeyens, L. (1997) Iron enrichment experiments in the Southern Ocean: physiological responses of plankton communities. *Deep-Sea Res. II*, **44**, 189–207.

Van Oijen, T., Van Leeuwe, M. A. and Gieskes, W. W. C. (2003) Variation of particulate carbohydrate pools over time and depth in a diatom-dominated plankton community at the Antarctic Polar Front. *Polar Biol.*, **26**, 195–201.

Vårum, K. M., Østgaard, K. and Grimsrud, K. (1986) Diurnal rhythms in carbohydrate metabolism of the marine diatom *Skeletonema costatum* (Grev.) Cleve. *J. Exp. Mar. Biol. Ecol.*, **102**, 249–256.

APPENDIX

I. Intracellular carbon dynamics

We assume that the incorporation of carbon into the intracellular glucan pool is governed by the differential equation:

$$\frac{dC}{dt} = P - R \tag{2}$$

where C is the cellular glucan amount in carbon units and P and R are the production and respiration rate of glucan, respectively. P and R are assumed to be given by the constants P_d and R_d during the light period ($0 \leq t < 12$) and by $P_n = 0$ and R_n during the dark period ($12 \leq t < 24$). For the light period, (2) has the solution

$$C(t) = C_0 + (P_d - R_d)t \qquad (0 \leq t < 12) \tag{3}$$

where C_0 is the intracellular glucan content at the beginning of the light period. The cellular glucan content at the beginning of the dark period is $C_0^n = C_0 + (P_d - R_d) \cdot 12$, implying that the nocturnal solution of (2), $C(t) = C_0^n + (0 - R_n)(t - 12)$ can be written as

$$C(t) = C_0 + 12 \cdot (P_d - R_d + R_n) - R_n t \qquad (12 \leq t < 24) \tag{4}$$

As a consistency requirement, we imposed the restriction $P_d = R_d + R_n$, implying that the cellular glucan content at the end of the dark period equals that at the beginning of the light period [i.e. $C(24) = C(0) = C_0$].

II. Intracellular dynamics of ^{14}C

The dynamics of ^{14}C in the intracellular glucan pool is governed by the balance between ^{14}C uptake during production and ^{14}C losses due to respiration. Uptake of ^{14}C is proportional to $P_d \cdot {}^{14}C_{med}/C_{med}$ (Dring and Jewson, 1982), where ${}^{14}C_{med}$ and C_{med} are the concentration of labelled and total carbon in the external medium, respectively. Similarly, losses of ^{14}C are proportional to $R_d \cdot {}^{14}C(t)/C(t)$, where ${}^{14}C(t)$ and $C(t)$ are the intracellular concentrations of labelled and total carbon at $t = 12$. For the light period, we get:

$$\frac{d^{14}C}{dt} = P_d \cdot \frac{{}^{14}C_{med}}{C_{med}} - R_d \frac{{}^{14}C}{C} \tag{5}$$

which, upon insertion of (3) can be written as:

$$\frac{d^{14}C}{dt} = P_d \cdot \frac{{}^{14}C_{med}}{C_{med}} - R_d \cdot \frac{{}^{14}C}{C_0 + (P_d - R_d)t} \tag{6}$$

Equation (6) is a linear ordinary differential equation that can be solved by standard methods [e.g. (Edelstein-Keshet, 1988)]. For the initial condition ${}^{14}C(0) = 0$, the solution is

$${}^{14}C(t) = \frac{{}^{14}C_{med}}{C_{med}} \cdot C(t)\left[1 - \left(\frac{C_0}{C(t)}\right)^{\frac{P_d}{P_d - R_d}}\right] \qquad (0 \leq t < 12) \tag{7}$$

implying that the proportion of ^{14}C in the cellular carbon pool, ${}^{14}C(t)/C(t)$, asymptotically approaches

$^{14}C_{med}/C_{med}$, the proportion in the external medium. In the dark period, no carbon is assimilated, implying that the internal proportion of ^{14}C remains constant at $^{14}C(12)/C(12)$. Accordingly, ^{14}C is lost at the same rate as C, implying

$$^{14}C(t) = \frac{^{14}C(12)}{C(12)} \cdot C(t) \qquad (12 \le t < 24) \qquad (8)$$

III. Total concentration of C and ^{14}C

To obtain the total amount of C at time t, $C_{tot}(t)$, the carbon content per cell, $C(t)$, has to be multiplied by $N(t)$, the number of cells at time t. We assume that the cell population grows exponentially with growth rate μ, i.e. $N(t) = N_0 e^{\mu t}$, implying

$$C_{tot}(t) = N_0 C(t) e^{\mu t} = N_0 e^{\mu t}[C_0 + (P - R)t] \qquad (9)$$

There is, however, a potential problem with this formulation, since it implicitly assumes that all cells have the same intracellular carbon dynamics, thereby neglecting age differences between cells. Assume, for example, that all cells that are produced anew start with a carbon content C_0. At the start of the day ($t = 0$), all N_0 cells have a carbon content C_0 and the carbon content of these preexisting cells is $C(T) = C_0 + (P - R)T$ at time T. However, at time T there are also other cells present that have been newly produced in the time interval $[0,T]$. Consider those cells which are of age t $(0 < t < T)$ at time T and, hence, were produced $T - t$ time units ago. These cells were, at that time, produced at a rate $\mu N(T - t) = \mu \cdot N_0 e^{\mu(T-t)}$ and they have, at time T, achieved an intracellular carbon concentration $C(t) = C_0 + (P - R)t$. The average intracellular carbon concentration $\bar{C}(T)$ of all the various age classes is given by:

$$\bar{C}(T) = \frac{N_0 C(T) + \int_0^T \mu N(T - t) C(t) dt}{N_0 + \int_0^T \mu N(T - t) dt} \qquad (10)$$

Inserting the terms for $N(T - t)$ and $C(t)$ and simplifying yields

$$\bar{C}(T) = \frac{N_0[C_0 + (P - R)T] + \int_0^T \mu e^{\mu(T-t)}[C_0 + (P - R)t] dt}{N_0 e^{\mu T}} \qquad (11)$$

which, after integration, further simplifies to

$$\bar{C}(T) = C_0 + (P - R)\frac{1}{\mu}(1 - e^{-\mu T}) \qquad (12)$$

If $\mu T << 1$, the last term in (12) is close to T:

$$\frac{1}{\mu}(1 - e^{-\mu T}) \approx T \quad \text{for } \mu T << 1 \qquad (13)$$

implying that $\bar{C}(T) \approx C_0 + (P - R)T = C(T)$. Hence in a slowly growing population, age structure has a negligible effect on the cellular carbon dynamics. For larger values of μ, equation (9) for carbon concentration at time t should be replaced by

$$C_{tot}(t) = N(t) \cdot \bar{C}(t) = N_0 e^{\mu t}\left[C_0 + (P - R)\frac{1}{\mu}(1 - e^{-\mu t})\right] \qquad (14)$$

Similarly, the ^{14}C dynamics can be affected by age structure implying that the C in equation (5) has to be replaced by $\bar{C}$. However, for our parameter constellation equations (5) and (9) provide reasonable approximations.